Dynamic Analysis of Wind Turbines Considering New Grid Code Requirements

M.B.C. Salles[1,2], K. Hameyer[1], J.R. Cardoso[2], W. Freitas[3] , *Members* IEEE
[1]Institute of Electrical Machines - IEM, RWTH Aachen University, Germany
[2]Laboratory of Applied Electromagnetism - LMAG, University of São Paulo, Brazil
[3]Power System Department – DSEE, University of Campinas, Brazil
mauricio.salles@iem.rwth-aachen.de; mausalles@gmail.com

***Abstract*- E.ON Netz new grid code requires the ability from the wind turbines to remain connected to the network when terminal voltage level drops to zero for at least 150 ms. Moreover, wind turbines must also contribute with voltage regulation during and after grid faults. A comparative study analyzing the dynamic behavior of conventional versions of wind turbines based on doubly-fed induction generator and on permanent magnet synchronous generator is presented in this paper. Computational simulations have showed that wind turbine based on PMSG can contribute with more injection of reactive power to the network. The converters nominal power and the strategy of its current controllers can impact the dynamic behavior of wind turbines.**

***Index Terms*—dynamic modeling, doubly-fed induction generator, permanent magnet synchronous generator, wind turbines.**

I. Introduction

Usually, a wind turbine (WT) equipped with blade pitch angle control can generate more than 600 KW and are grouped in wind farms from about 40 MW to more than 150 MW in offshore installations. In 2005, 45% of the medium-large wind turbines installed in Europe were based on doubly-fed induction generators (DFIG) [1]. However the number of installed wind turbines based on permanent magnet synchronous generators (PMSG) is still very small [1].

In the last 10 years, the use of permanent magnet materials has been increasing considerably. This fact has contributed to the development of new concepts of electrical machines for new application [2],[3]. Comparative studies have showed that PMSG has many advantages when compared to the conventional DFIG or even with the synchronous generator with electrical excitation [3]. One of the reasons is the elimination of the gearbox between turbine rotor and generator rotor due to the several pole pars construction.

New grid codes require the ability from wind turbines to keep connected and to provide voltage support during and after grid faults [4],[7]. Different from the classical synchronous generator with field excitation, these two concepts are not able to be connected directly to the network or to inject reactive power to control terminal voltage without the use of two back-to-back converters [6],[7]. Despite the fact that similar operation of the back-to-back converters in both concepts has been used, wind turbines based on PMSG can contribute with more reactive power injection to the network during faults. The dependence on the converter capacity and on the adopted current control loop strategy will be discussed in this paper.

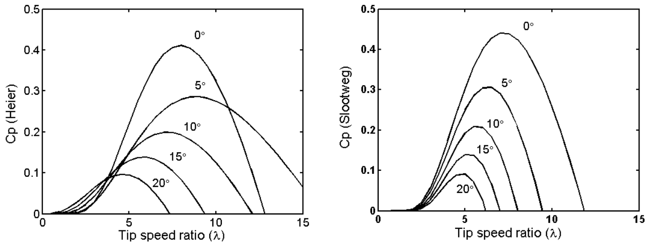

Fig. 1 Performance coefficient curves.

This paper is organized as follows. Section II shortly discusses the dynamic model of the wind turbine. Section III presents a brief description of the DFIG. The PMSG is described in Section IV. The dynamic analyses of both concepts are presented in Section V. In Section VI, the E.ON Netz Grid Code is presented and some main points are discussed in Section VII.

II. Wind Turbine Dynamic Model

The mechanical power capture from the wind can be calculated using the well-know aerodynamic equation [5],[6]:

$$P_m = \frac{1}{2} A \rho V^3 C_P(\lambda, \beta) \tag{1}$$

where A is the turbine rotor area, ρ is the density of the air, V is the wind speed, C_p is the performance coefficient, β is the blade pitch angle, $\lambda = \omega R/V$ is the tip speed ratio, R is the radius of the rotor and ω is the mechanical angular speed of the blades. The performance coefficient depends on the blade pitch angle and on the tip speed ratio (λ). Both concepts analyzed in this paper are modeled with pitch angle control [5].

Usually, a group of performance coefficient curves are experimentally determined by the manufactures for different pitch angle position and tip speed ratio. The implemented wind turbine model for the DFIG is suggested by Heier while for the PMSG is suggested by Slootweg [5]. The last model was chosen for the PMSG because it represents better the aerodynamic of modern wind turbines.

One can see from the selected curves (Fig. 1) that the maximum value of Cp has been improved capturing more energy from the wind. Another important characteristic of modern wind turbines is the optimization of the maximum tip

978-1-4244-1736-0/08/$25.00

speed ratio (λ) values. This fact allows sparing the mechanical action of the blade pitch control and makes the generator speed control more effective.

III. Doubly-Fed Induction Generator

This is the most wide spread configuration of wind turbine since the development of highly efficient power electronics [1]. This concept consists in two back-to-back voltage source converters connecting the grid and the rotor windings. Stator circuits are connected direct to the grid (Fig. 2). The parameters of the DFIG used in this analysis can be found in [5]. Its speed range is up to 0.7 to 1.31 pu of the synchronous speed. The variable speed operation makes possible the maximization of the performance coefficient (*Cp*) for different wind speeds. The rotor-side converter control regulates the rotor speed to its optimum value.

A. Rotor-Side Converter

In normal operation, rotor-side converter regulates the developed electric power (P_{elec}) and the absorbed reactive power by the DFIG. In Fig. 3 the control adopted here is depicted. The encoder gives the generator rotor position (θ) to the abc-dq0 and to the dq0-abc transformations.

The direct axis component is used to regulate the generator power factor to 1 pu thus, the absorbed reactive power reference (Q^*) is equal to 0 (zero). The actual absorbed reactive power at the grid connection (Q) of the DFIG is compared to the reference and the error is sent to first PI (Proportional Integral) controller to determine the reference current (I^*d) for the direct axis component. The I^*d is compared to the actual value of Id and the error is sent to the second PI controller to determine the reference voltage (V^*d) for the direct axis component.

The quadrature axis component is controlled similarly to the direct axis, however, it regulates the electric power to the optimal reference (P^*_{opt}). After a dq0-to-abc transformation, the V^*d and the V^*q are sent to the PWM (Pulse-width Modulation) signal generator. Finally, V^*abcr are the three-phase voltages desired at the rotor-side converter output. The IGBT's (Insulated Gate Bipolar Transistor) are considered ideals and its commutation are neglected.

B. Grid-Side Converter

In normal operation, the voltage of the direct-current link (DC link) between both converters is controlled by the grid side-converter (Fig. 4). Such controller employs a PLL (Phase Locked Loop) providing the angle (ϕ) to the abc-to-dq0 (and dq0-to-abc) transformation to synchronize the three-phase voltages at the converter output with the zero crossings of the fundamental component of the phase-A grid voltage.

The direct axis component is used to regulate DC link voltage (V^*dc) to 1 pu. The actual DC link voltage (Vdc) is compared to the reference and the error is sent to the first PI controller to determine the reference current (I^*d) for the direct axis component. The I^*d is compared to the actual value of Id and the error is sent to the second PI controller to determine the reference voltage (V^*d) for the direct axis component.

As in normal operation the rotor-side converter already regulates the power factor of the DFIG, the necessity of reactive power regulation by the grid-side converter is eliminated. Thus, the quadrature axis component of the reference current is set to 0 ($I^*q = 0$). The I^*q is compared to the actual value of Iq and the error is sent to the first PI controller to determine the reference voltage (V^*q) for the quadrature axis component. After a dq0-to-abc transformation, the V^*d and the V^*q are sent to the PWM signal generator. Finally, $V^*abc\_grid\_conv$ are the three-phase voltages desired at the grid-side converter output.

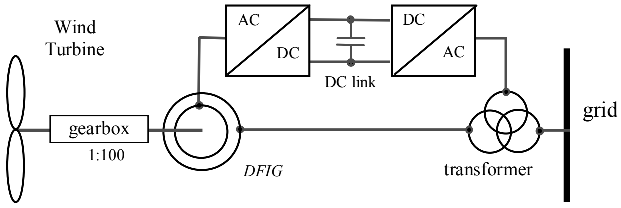

Fig. 2 Doubly-fed induction generator (DFIG).

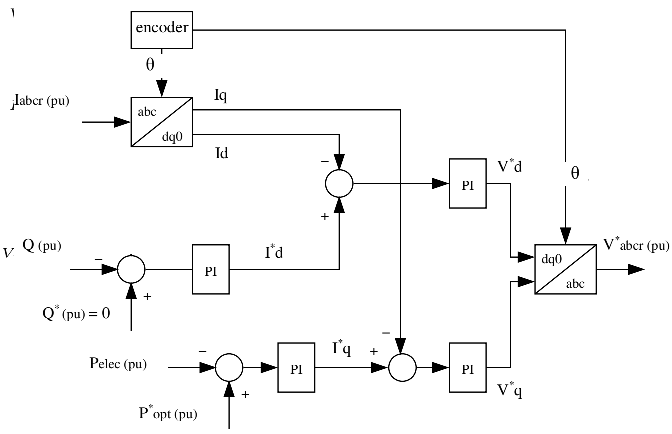

Fig. 3 Rotor-side control diagram for DFIG in normal operation.

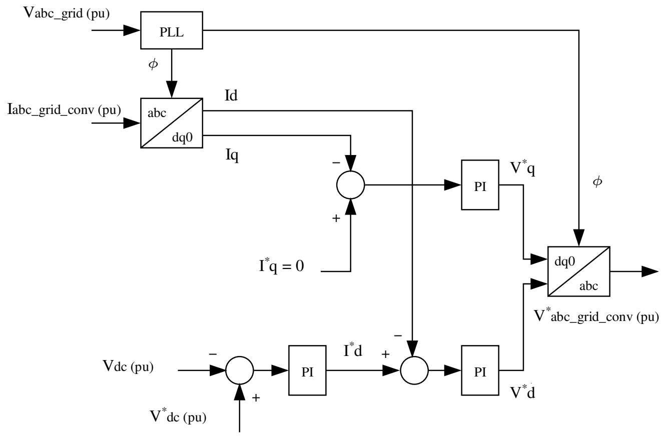

Fig. 4 Grid-side control diagram for DFIG in normal operation.

C. Operation of DFIG During Grid Faults

To accomplish with the new grid codes requirements some methodologies has been proposed in the literature [7]-[9]. As the stator of the DFIG is connected direct to the grid, some undesirable high currents may be induced in the rotor windings and the protection system may block the rotor-side converter. Therefore, in this model when the terminal voltage drops below 0.9 pu the rotor-side converter stops controlling power factor and the grid-side converter starts controlling grid terminal voltage via an additional current loop controller (Fig. 7).

IV. Permanent Magnet Synchronous Generator

The conventional inner rotor radial-flux PMSG was found to be the most suitable machine for gearless wind turbines when compared with different concepts [3]. The stator of this machine is connected to the grid through two back-to-back voltage source converters, it is similar to the DFIG converter however with full capacity (Fig. 5). The generator parameters of the PMSG used in this analysis can be found in [10]. Its speed range is up to 9 to 21.7 rpm.

A. Generator-Side Converter

In normal operation, generator-side converter regulates the optimal generator rotor speed ($\omega_r^* opt$) and could regulates the generator power factor to unitary value (Fig. 6). The encoder gives the generator rotor position (θ) to the dq0-abc transformation. The direct axis component could be used to regulate the generator power factor, however, only active power from the generator can be inject into the grid. Therefore, the direct axis component of the reference current (I^*d) is set to 0 (zero) to simplify the control loop and to give maximum electromagnetic torque (T_e) [11],[12]. The quadrature axis component of the current (Iq) is used to regulate the generator actual speed (ω_r) to the optimum speed ($\omega_r^* opt$). The actual generator speed is compared to the optimum speed and the error is sent to a PI controller to determine the current reference (I^*q). After a dq0-to-abc transformation, the three-phase reference currents (I^*abcs) are compared at the current controller to the actual values ($Iabcs$) and sent to the PWM. Finally, V^*abcs are the three-phase voltages desired at the rotor-side converter output.

B. Grid-Side Converter

In normal operation the grid-side converter is controlled in the same way as the DFIG grid-side converter (Fig. 4) including a current controller loop to regulate the terminal voltage (Fig. 7). The quadrature axis component of the current (Iq) is used to regulate the terminal voltage (Vt) to the reference value (Vt^*). The actual terminal voltage is compared to the reference and the error is sent to the first PI controller to determine the reference current (I^*q). This current loop controller also includes a droop characteristic of 2%. The following stages of the control are already described in subsection B of Section III.

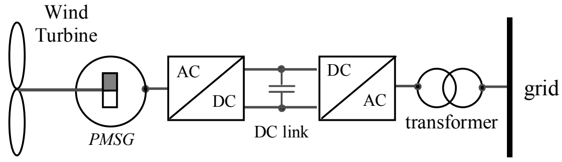

Fig. 5 Permanent magnet synchronous generator (PMSG).

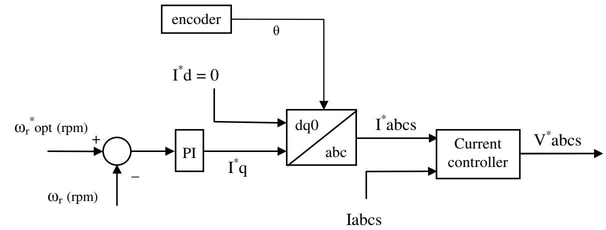

Fig. 6 Generator-side control diagram for PMSG in normal operation.

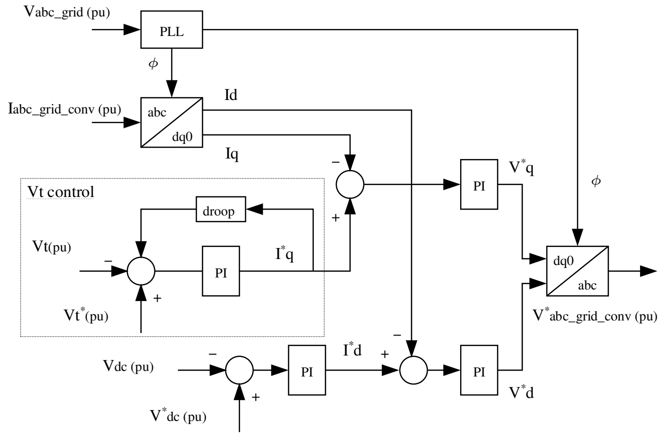

Fig. 7 Grid-side control diagram for PMSG in normal operation.

C. Operation of PMSG During Grid Faults

To accomplish with the new grid codes requirements some methodologies has been proposed [10],[13]. PMSG is different from the DFIG considering the way that the converter feeds the grid. The DFIG the stator is connected directly to the grid and the partial grid-side converter feeds generator stator and grid with active and reactive power. The PMSG grid-side converter feeds only the grid. This converter requires full power and must have more than 100% of the generator rated power to control power factor or terminal voltage when the wind speed is higher than nominal. In this model, a current priority strategy is used in order to analyze the dynamic behavior of the reactive and the active power during grid faults.

V. Dynamic Analysis Of Wind Turbines

In this section, the investigation of the dynamic behavior of wind turbines during a 150ms grid fault which makes the voltage level of the PCC (Point of Common Coupling) drop to approximately 0.6 pu. The wind farm is connected to the PCC through a 30 km single 3-phase line. The results are presented in the following subsections.

A. DFIG Dynamic Analysis

The 9 MW wind farm based on DFIG is equipped with 6 wind turbines. This analysis is performed taking into account different converter capacities (25%, 35% and 50% of the generator rated power). The most important variables are presented from Fig. 8 to Fig. 13. It can be noted that in Fig. 8 the terminal voltage level assumes higher value when the converter capacity is 50% of the DFIG rated power. This fact could be explained by the injection of reactive power into the grid (Fig. 9). For 25% or 35% converters the generator stator consumes more reactive power than the converter could supply during the fault and it takes this difference from the grid. The injection of reactive power into the grid is only possible for the 50% converter. The injection of the reactive power by the grid-side converters are showed in Fig. 10, the are limited by the rated capacity of the converter taking into account also the I^*d reference current which controls the dc link voltage.

The terminal voltage level also influences directly the active power injection and the rotor speed. The injected active power is 0.75 pu when the capacity of the converter is 50% of rated power while it is 0.62 pu for the converter with 25% capacity (Fig. 11). The rotor speed reaches higher values for lower values of terminal voltage (Fig. 12) consuming more reactive power from the grid. The pitch angle control also actuates slightly less for the DFIG with 50% of the rated power (Fig. 13).

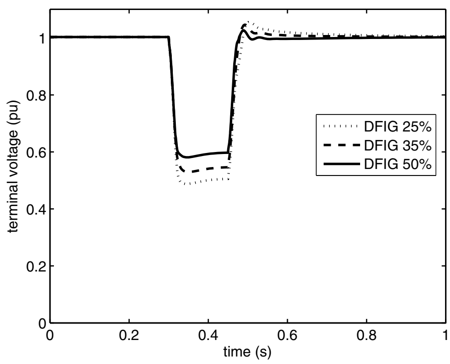

Fig. 8 Terminal voltage of the wind farm based on DFIG.

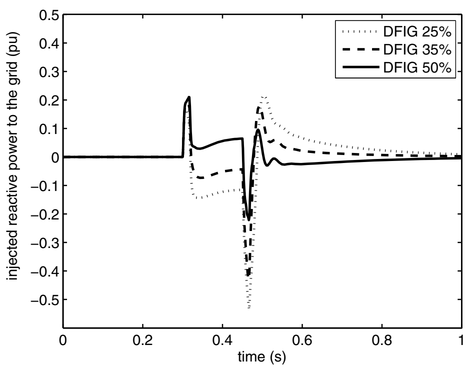

Fig. 9 Reactive power injected by the wind farm based on DFIG.

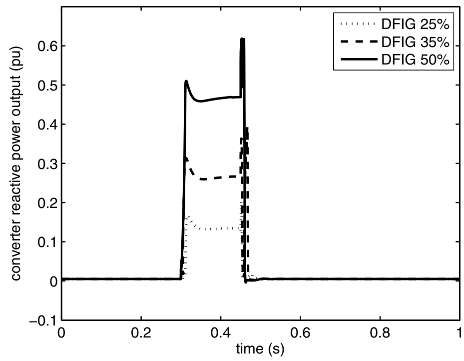

Fig. 10 Reactive power inject by the grid-side converter of the DFIG.

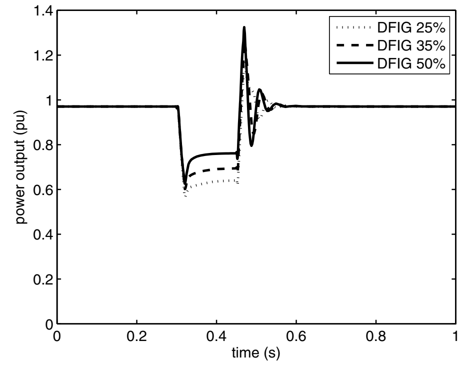

Fig. 11 Active power injected by the wind farm based on DFIG.

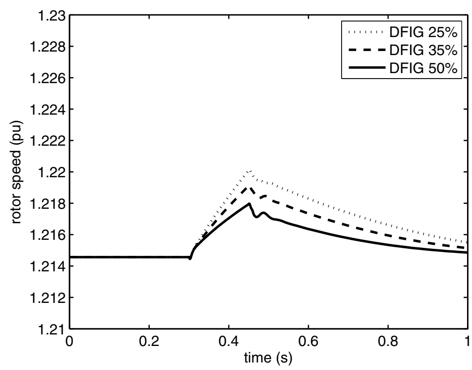

Fig. 12 Rotor speed of the wind turbine based on DFIG.

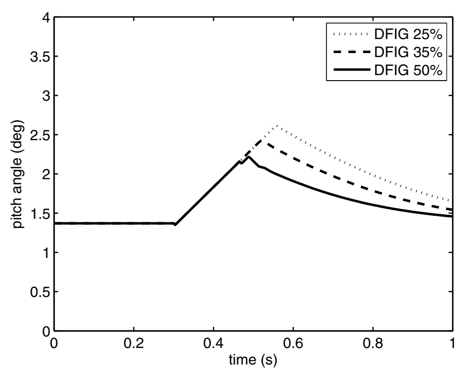

Fig. 13 Blade pitch angle position of the wind turbine based on DFIG.

B. PMSG Dynamic Analysis

The 10 MW wind farm based on PMSG is equipped with 5 wind turbines. The capacity of the implemented converter is 110% of the PMSG rated power in order to enable the ability of controlling terminal voltage during nominal active power injection. Even a higher capacity of the converter is suggested in a recent study about voltage and transient stability support [13]. The simulation here are performed taking into account a current control priority strategy that gives the priority in the total reference current of the grid-side converter ($I^{*}conv = 1.1\ pu$) to one current controller loop $I^{*}d$ or $I^{*}q$. Using the equation (2) the not priorized reference current is calculated. The most important variables are presented from Fig. 14 to Fig. 17 where the term "no priority" means also no limit for $I^{*}conv$.

$$I^{*}conv = \sqrt{\left(I^{*}d\right)^{2} + \left(I^{*}q\right)^{2}} \qquad (2)$$

In Fig. 14, it can be noted that the voltage level at the wind farm terminals reaches the highest value for the case using the $I^{*}q$ priority. This fact can be explained analyzing Fig. 15 where the highest injection of reactive power is due to no current priority strategy. The highest values terminal voltage and reactive power do not coincide since the 30 km line is overloaded for no current priority. In this case, the apparent current injected by the grid-side converter reaches almost 1.8 pu and the terminal voltage drops. The rotor speed and the pitch angle position do no change during the fault, and in consequence of that the injected active power from the generator to the generator-side converter does not change. The unbalance between the injected active power from the generator and the injected active power to the grid during the grid fault makes the voltage at the dc link drop (Fig. 17). The energy not injected into the grid during the fault is injected immediately after the fault extinction (as one can see in Fig. 16) and the dc link voltage starts to recover. Between other methodologies, this problem could be overcome controlling also the electrical power of the generator during grid faults or introducing an active dc link. For more severe faults the generator may be disconnected and reconnected after the fault elimination [10].

VI. E.ON NETZ GRID CODE REQUIREMENTS

E.ON Netz is one of the German Transmission System Operators that in its 2006 grid code [4] requires the wind farms not to disconnect during unlimited time when the voltage at the PCC drops below 80% of the nominal voltage. Also when the PCC voltage is zero the wind farms must be connected within 150ms. Only in specific circumstances short term interruption (STI) is allowed (Fig. 18). For voltage regulation, this German grid code requires the wind farm to supply at least 100% of reactive current when the voltage drops below 50%. A dead band is included around the reference voltage in which the control should actuate as power factor control (Fig. 19).

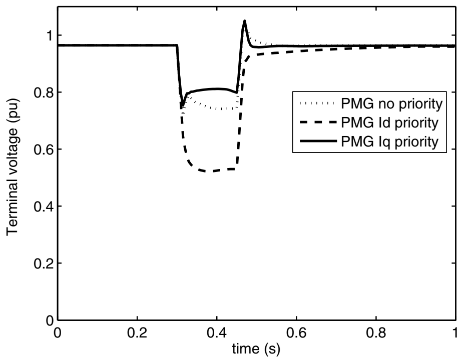

Fig. 14 Terminal voltage of the wind farm based on PMSG.

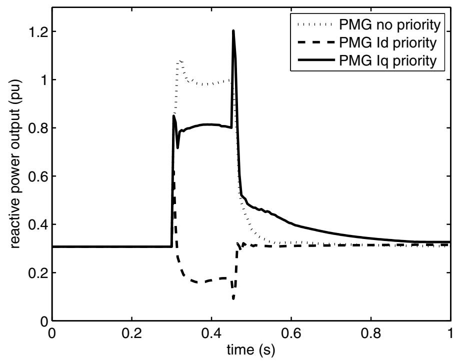

Fig. 15 Reactive power injected by the grid-side converter of the PMSG.

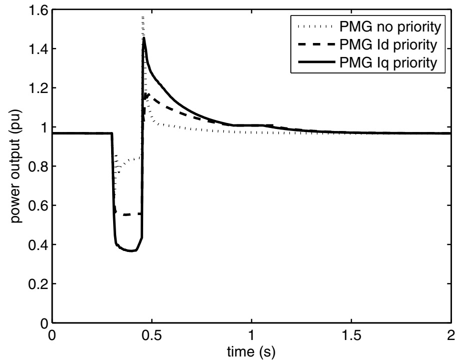

Fig. 16 Active power injected by the wind farm based on PMSG.

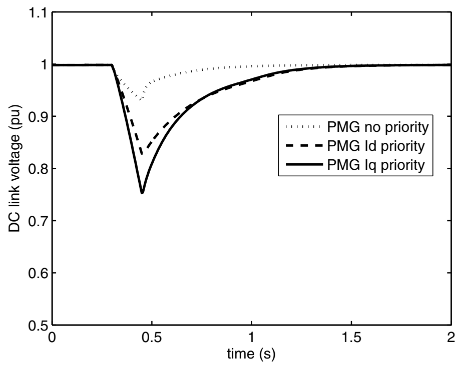

Fig. 17 Voltage of the DC link of the wind turbine based on PMSG.

The requirements presented here are the most restricted among the others transmission system grid codes from countries that already have high wind energy penetration like Spain, Denmark and Ireland.

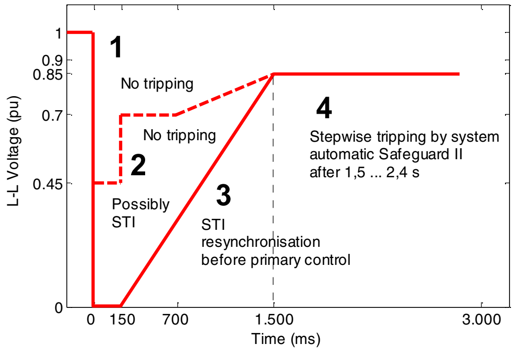

Fig. 18 E.ON Netz fault-ride through requirements (reproduction).

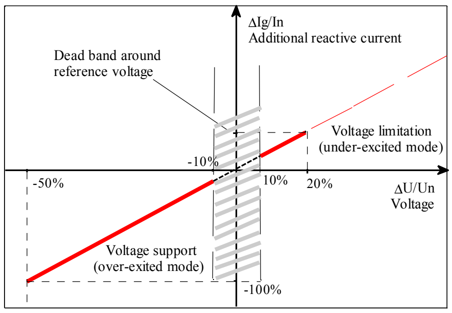

Fig. 19 E.ON Netz voltage regulation requirements (reproduction).

VII. Discussions

This paper presents the dynamic model and the analysis of two different wind turbine technologies during a grid fault that makes the voltage drop to 0.6 pu at the PCC of a wind farm. The average version of the DFIG and the PMSG implemented in these studies do not accomplish with the E.ON Netz grid code voltage support requirements. However, for the simulated gird fault the fault-ride through capability requirement is filled by both technologies.

Not only for the results obtained here but also taking into account the results discussed in many of the references we conclude that the DFIG needs to have additional reactive power reserves to be able to inject 100% of rated power into the grid during PCC voltage drops. Some extra investments should be done. The PMSG could be adapted more easily to the requirements with some modifications.

The DFIG and the PMSG can be adapted to accomplish to the fault-ride through requirements, therefore another options that before this new requirements was not sufficiently interesting could increase its market share. One example is the squirrel-cage induction generator connected to the grid via full-load converter enabling the variable speed operation [14]. Moreover, the use of FACTS (Flexible Alternating Current Transmission System) at the PCC has become even more interesting than before.

Acknowledgment

The authors gratefully acknowledge the financial support from Brazil by FAPESP ("Fundação de Amparo à Pesquisa do Estado de São Paulo"), by CNPq ("Conselho Nacional de Desenvolvimento Científico e Tecnológico") and by CAPES ("Coordenação de Aperfeiçoamento de Pessoal de Nível Superior") and also from Germany by DAAD ("Deutscher Akademischer Austausch Dienst") to develop this research.

References

[1] European Wind Energy Association, "*Large Scale Integration Of Wind Energy In The European Power Supply: analysis, issues and recommendations*." Technical Report, December, 2005.

[2] M. R. Dubois, *Optimized Permanent Magnet Generator Topologies for Direct-Drive Wind Turbines*, PhD thesis, Delft University of Technology, Delft, The Netherlands, 2004.

[3] Polinder, H.; van der Pijl, F.F.A.; de Vilder, G.-J.; Tavner, P.J.; "Comparison of direct-drive and geared generator concepts for wind turbines", *IEEE Transactions on Energy Conversion*, vol. 21, no. 3, pp. 725-733, 2006.

[4] Grid Code: High and Extra High Voltage, E.ON Netz GmbH Tech. Rep., 2006, Status:1.

[5] J. G. Slootweg; H. Polinder; W. L. Kling, "Representing Wind Turbine Electrical Generating Systems in Fundamental Frequency Simulations", *IEEE Transactions on Energy Conversion*, vol. 18, no.4, pp. 516–524, 2003.

[6] Siegfreied Heier, "*Grid Integration of Wind Energy Conversion Systems*", 2nd ed., John Wiley & Sons, England, 2006.

[7] V. Akhmatov, "*Analysis of Dynamic Behaviour of Electric Power Systems with Large Amount of Wind Power*", Ph.D. thesis, Technical Univ. of Denmark, Lyngby, Denmark, 2003.

[8] J. Morren, S.W.H de Haan, "Ridethrough of wind turbines with doubly-fed induction generator during a voltage dip", *IEEE Transactions on Energy Conversion*, vol. 20, no. 2, pp. 435-441, 2005.

[9] Dawei Zhi; Lie Xu; "Direct Power Control of DFIG with Constant Switching Frequency and Improved Transient Performance", *IEEE Transactions on Energy Conversion*, vol. 22, no. 1, pp. 110-118, 2007.

[10] V. Akhmatov, "Modelling and Ride-through Capability of Variable Speed Wind Turbines with Permanent Magnet Generators", *Wind Energy*, Vol. 9, No. 4, pp. 313-326, 2006.

[11] S. Morimoto, Y. Takeda, T. Hirasa, "Current phase control methods for permanent magnet synchronous motors", *IEEE Transactions on Power Electronics*, vol. 5, no.2, pp. 133–139, 1990.

[12] M.N. Uddin, T.S. Radwan, G.H. George, M.A. Rahman, "Performance of Current Controllers for VSI-fed IPMSM Drive", *IEEE Transactions on Industry Applications*, vol. 36, no.5, pp. 1531–1538, 2000.

[13] N.R. Ullah, T. Thiringer, D. Karlsson, "Voltage and Transient Stability Support by Wind Farms Complying With the E.ON Netz Grid Code", *IEEE Transactions on Power Systems*, vol. 22, no. 4, pp. 1647-1656, 2007.

[14] V. Akhmatov, "Full-load Converter Connected Asynchronous Generators for MW Class Wind Turbines", *Wind Engineering*, vol. 29, no. 4, pp. 341-351(11), 2005.